UC Irvine
UC Irvine Previously Published Works

Title
Impacts of the Indian Ocean on the ENSO cycle

Permalink
https://escholarship.org/uc/item/7kt469r8

Journal
Geophysical Research Letters, 29(8)

ISSN
0094-8276

Authors
Yu, JY
Mechoso, CR
McWilliams, JC
et al.

Publication Date
2002-04-15

Copyright Information

Peer reviewed

Impacts of the Indian Ocean on the ENSO cycle

Jin-Yi Yu, Carlos R. Mechoso, James C. McWilliams, and Akio Arakawa

Department of Atmospheric Sciences, University of California, Los Angeles, USA

[1]   This study examines the impacts of the Indian Ocean on the ENSO (El Niño-Southern Oscillation) cycle by performing experiments with a coupled atmosphere-ocean general circulation model (CGCM). In one of the experiments, the ocean model domain includes only the tropical Pacific Ocean (the Pacific Run). In the other experiment, the ocean model domain includes both the Indian and tropical Pacific Oceans (the Indo-Pacific Run). The experiment results show that the CGCM simulation of ENSO including both the Indian and tropical Pacific Oceans tends to be more realistic than that including the tropical Pacific Ocean only. In particular, the Indo-Pacific Run produces ENSO events with larger amplitude and greater variability on decadal time scales. The interactive Indian Ocean also affects the surface heat flux anomalies in the Indian Ocean during the ENSO cycle and surface wind stress anomalies in both the tropical Indian and Pacific Oceans. There are indications that both surface heat flux and wind stress are actively forcing a portion of the interannual variability in the Indian Ocean during the ENSO cycle.   *INDEX TERMS:* 1620 Global Change: Climate dynamics (3309); 4522 Oceanography: Physical: El Niño; 3339 Meteorology and Atmospheric Dynamics: Ocean/atmosphere interactions (0312, 4504); 4504 Oceanography: Physical: Air/sea interactions (0312)

1.   Introduction

[2]   It has been suggested that variations in the Indian Ocean can influence ENSO (El Niño-Southern Oscillation) either through the atmosphere or the ocean. The proposed mechanism that supports the atmospheric connection recognizes the co-location of the rising zone of the transverse circulation components of the Indian Monsoon and the ascending branch of the Walker circulation [*Webster et al.*, 1992]. Variations in the strength of the monsoon can influence those in the Pacific trade winds and, consequently, the period and magnitude of ENSO [*Barnett*, 1984; *Wainer and Webster*, 1996]. The proposed mechanism that supports the oceanic connection assigns a key role to the Indonesian throughflow. Since ENSO manifests itself as an eastward displacement of warm water from the western to the eastern equatorial Pacific, the throughflow could modulate the warm pool in the western Pacific [*Wyrtki*, 1987] and thus influence the period and magnitude of ENSO [*Philander and Delecluse*, 1983]. It has also been suggested that ENSO events can impact the atmosphere-ocean system over the Indian Ocean. *Klein et al.* [1999] showed from observations that sea surface temperature (SST) anomalies usually appear in the Indian Ocean during ENSO events through an ''atmospheric bridge'' mechanism [*Lau and Nath*, 1996]. It is possible that remote ENSO effects are amplified by air-sea interactions in the Indian Ocean and in turn affect ENSO activity through the atmosphere and/or the ocean.

[3]   The present study aims to examine the impacts of the Indian Ocean on the ENSO cycle and its associated ocean–atmosphere fluxes over the Indo-Pacific Ocean region. Two long-term simula-

tions have been performed with the UCLA coupled atmosphere-ocean general circulation model (CGCM). In the first CGCM simulation, the oceanic component of the CGCM includes only the tropical Pacific Ocean (Pacific Run, hereafter). In the second CGCM simulation, the oceanic component includes both the tropical Pacific and Indian Oceans (Indo-Pacific Run, hereafter). The climate variability produced in these two CGCM runs are contrasted.

2.   Model and Simulation

[4]   The UCLA CGCM consists of the UCLA atmospheric GCM (AGCM) and the GFDL Modular Ocean Model (MOM). The AGCM is global with a horizontal resolution of 5°-longitude by 4°-latitude and 15 levels in the vertical. Figure 1 shows the oceanic domains covered by MOM in the Pacific and Indo-Pacific Runs. The oceanic model has a longitudinal resolution of 1°, a latitudinal resolution that varies gradually from 1/3° between 10°S and 10°N to about 3° at both 30°S and 50°N, and 27 layers in the vertical. Outside the oceanic model domain, SSTs for the AGCM are prescribed based on a monthly SST climatology [*Alexander and Mobley*, 1976]. The Pacific and Indo-Pacific Runs are both integrated for 52 years. Only the results after year 10 are analyzed in this paper. The long-term mean SSTs simulated by these two CGCM runs are shown in Figure 1. Both runs produce reasonably realistic simulations of the mean SSTs in the Pacific and Indian Oceans, with a warm pool (SST greater than 28°C) that covers both the tropical western Pacific and the eastern Indian Oceans and a cold tongue that covers the eastern equatorial Pacific.

3.   Impacts on ENSO Activity

[5]   Figure 2 compares the interannual variability of equatorial SST produced by the two CGCM runs. These values are obtained by removing the long-term mean annual cycle and the contributions of timescales shorter than one year. The Pacific Run produces warm events approximately every 3–5 years (Figure 2a). The maximum SST anomalies in the strongest El Niño event are about 2°C at year 25. The spatial structures and temporal evolutions of warm and cold events have been examined by *Yu and Mechoso* [2001]. The Indo-Pacific Run produces a stronger interannual variability in the equatorial Pacific (Figure 2b). The maximum SST anomalies in the strongest El Niño event (at Year 12) are about 3°C. Figure 3 compares the time series of the NINO3 index (SST anomalies averaged between 90°–150°W and between 5°S–5°N) calculated from the two CGCM runs with the NINO3 indices observed during 1955–2000. The standard deviation of the NINO3 index is 0.78°C for the Indo-Pacific Run, 0.50°C for the Pacific Run, and 0.77°C for the observations. It is also noticed that the Indo-Pacific Run has a greater decadal variation in ENSO intensity than the Pacific Run. The former run can be broadly separated into two ''strong variability decades'' (Years 10–21 and 38–52) with large warm and cold events and a ''weak variability decade'' (Years 22–37) with weak warm and cold events. No such clear decadal differences are present in the Pacific Run. It appears that by including the Indian Ocean, the CGCM produces a more realistic ENSO amplitude and stronger variability on decadal timescales.

[6]   To examine the ENSO cycle, we apply the Multi-Channel Singular Spectrum Analysis (M-SSA) [*Keppenne and Ghil*, 1992]
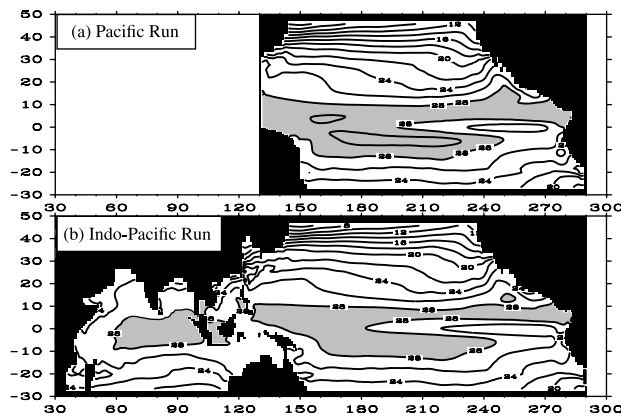
Figure 1. Ocean model domains used in the (a) Pacific Run and (b) Indo-Pacific Run. Also shown are the long-term mean SSTs produced by these two runs. Contour intervals are 2. Values greater than 28 are shaded.

simultaneously to SST, surface wind stress and surface heat flux anomalies in the Indo-Pacific Ocean domain produced by the two CGCM simulations and to those obtained from the *Atlas of Surface Marine Data 1994* compiled by *da Silva et al.* [1994]. The analyses presented in the atlas are derived from the individual observations found in the Compressed Marine Reports-Product 5 (CMR-5) of COADS Release 1 [*Slutz et al.*, 1985; *Woodruff et al.*, 1987]. The atlas provides analyzed monthly anomalies from January 1945 to December 1993. Only the anomalies during 1964–1993 are used here for M-SSA analysis.
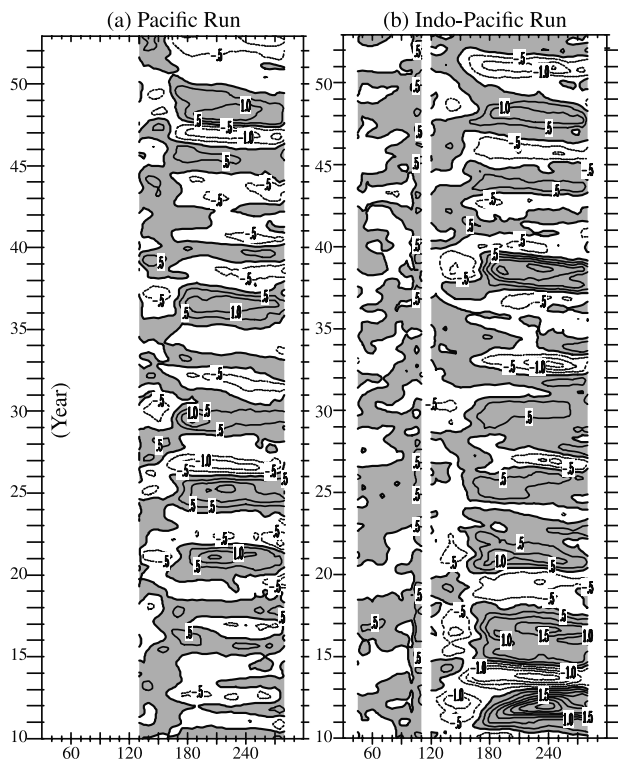

Figure 2. Interannual variability of SST along the equatorial Indo-Pacific Oceans produced from the (a) Pacific Run and (b) Indo-Pacific Run. Annual cycles are removed, and a low-pass filter is applied to remove variability with timescales less than 12 months. Contour intervals are 0.5. Positive values are shaded.
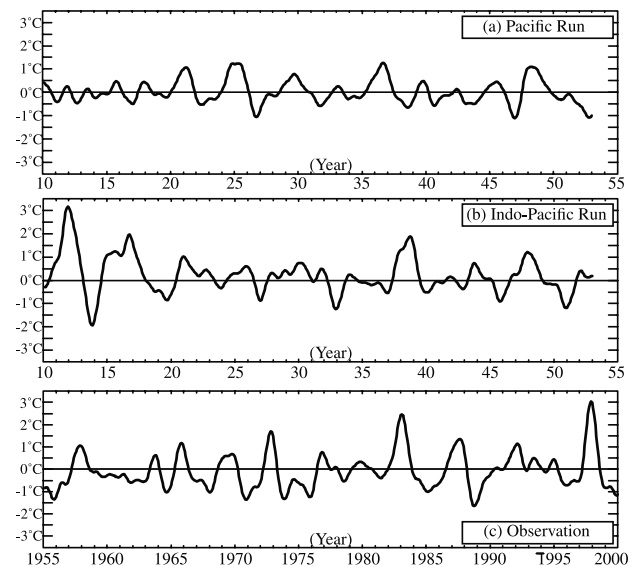

Figure 3. NINO3 indices calculated from (a) the Pacific Run, (b) the Indo-Pacific Run, and (c) the observations. These monthly values are low-pass filtered to remove variations shorter than 12 months.

[7] Figure 4 shows the eigenvector structures of SST anomalies corresponding to the leading oscillatory modes (i.e., the ENSO cycle) along the equator from the CGCM runs and the atlas data. It shows that the dominant period of the simulated ENSO cycle increases from about 4 years in the Pacific Run to about 4.4 years in the Indo-Pacific Run. The atlas data shows a dominant 4-year period for ENSO events during 1964–1993. SST anomalies during ENSO events show a slow westward propagation in the Pacific Run and are almost stationary in the Indo-Pacific Run and the atlas data. In addition, the centers of largest SST anomalies are located more toward the eastern Pacific in the Indo-Pacific Run, closer to those of the atlas data than the Pacific Run. The dominant time-scales, propagation features, and centers of SST anomalies of the simulated ENSO cycle are apparently affected by including an interactive Indian Ocean in the CGCM. The Indo-Pacific Run produces significant SST anomalies in the equatorial Indian Ocean during the ENSO cycle. These anomalies are characterized by a general warming (cooling) of the Indian ocean during the warm (cold) phase of the ENSO cycle. This is similar to the Indian Ocean SST anomalies revealed by the M-SSA analysis of the atlas data, except that the Indo-Pacific Run shows a larger east-west SST anomaly contrast. This may be related to the fact that both CGCM simulations produce stronger than observed SST anomalies in the western equatorial Pacific during the ENSO cycle. These anoma-lies may leak regionally into the eastern Indian Ocean as suggested by *Meyers* [1996].

4. Impacts on Ocean–Atmosphere Fluxes

[8] Figure 5 contrasts the surface heat flux and zonal wind stress anomalies of the leading oscillatory modes along the equator. Figures 5a–5c show that the surface heat anomalies produced by the two CGCM runs are similar in the Pacific Ocean but very different in the Indian Ocean. Over the Pacific sector, negative (positive) anomalies are produced in response to the warm (cold) phase of the ENSO cycle (compare Figures 4 and 5). These anomaly features are similar to those revealed by the atlas data (Figure 5c). In the Pacific Run over the Indian Ocean, surface heat flux anomalies are larger than and of opposite sign to those in the atlas data. The anomalies in the Pacific Run are particularly large over the western Indian Ocean. On the other hand, the Indo-Pacific
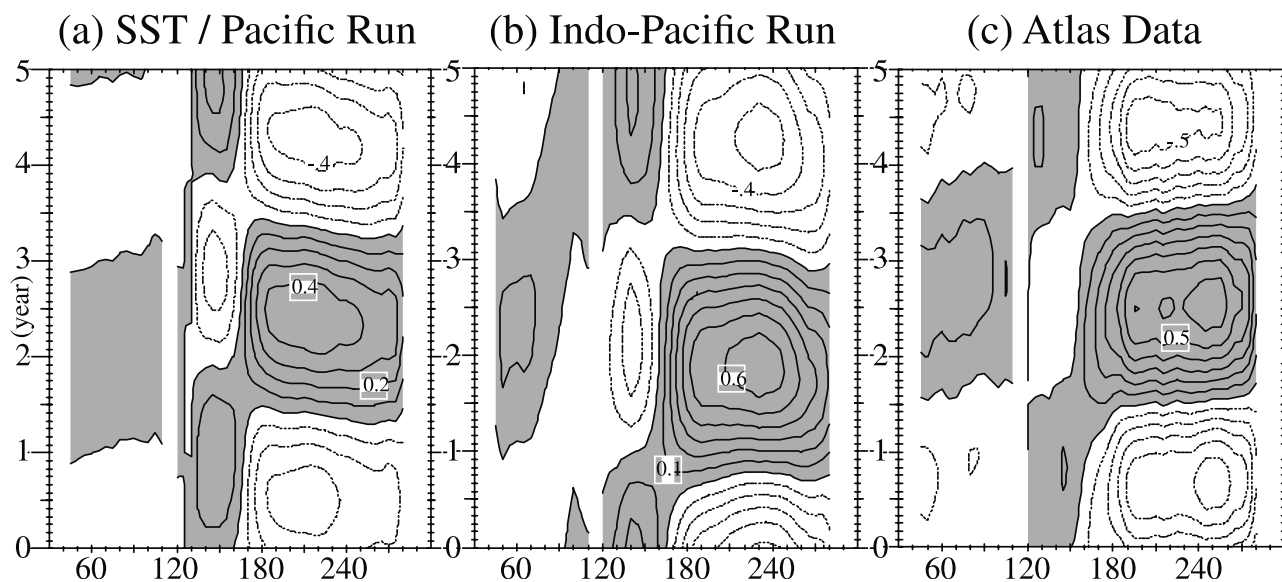
Figure 4. The eigenvector structures of SST anomalies along the equator for the leading oscillatory modes obtained by applying the combined 3-variable M-SSA analysis to (a) the Pacific Run, (b) the Indo-Pacific Run, and (c) the Atlas of Surface Marine Data 1994. The coordinate is the 61-month lag used in M-SSA. Contour intervals are 0.1 for SST. Positive values are shaded.

Run tends to produce more realistic surface heat flux anomalies in the Indian Ocean, with anomalies that are small and of the same sign as those of the atlas data.

[9] Figures 5d–5f show that the Pacific and Indo-Pacific Runs produce different zonal wind stress anomalies in both the Pacific and Indian Oceans. In the Pacific Run over the Pacific sector, zonal wind stress anomalies are established almost simultaneously along the equator during the mature phase of ENSO (Figure 5d). In the Indo-Pacific Run, the anomalies develop first in the western Pacific and then slowly propagate eastward (Figure 5e). A similar propagation of wind stress anomalies is seen in the atlas data (Figure 5f). Over the Indian Ocean, wind stress anomalies of opposite sign to those in the Pacific are produced in both CGCM runs. However, the anomalies produced in the Indo-Pacific run are much larger than those in the Pacific Run. The largest anomalies are located in the central Indian Ocean, which is similar to that of the atlas data.

[10] It is interesting to note that the center of large surface heat flux anomalies produced in the equatorial Indian Ocean by the Pacific Run (Figure 5a) coincides with the largest SST anomalies produced by the Indo-Pacific Run in the same region (Figure 4b). Figure 5a shows that positive surface heat flux anomalies are produced by the Pacific Run over the Indian Ocean during the warm ENSO phase, with the largest anomalies over the western part of the Indian Ocean. It suggests that the atmosphere tends to warm the ocean in this region. This is consistent with the warming of the western Indian Ocean SSTs produced by the Indo-Pacific Run. The resultant warm SSTs reduce surface heat fluxes and produce the small heat flux anomalies shown in the Indo-Pacific Run (Figure 5b). Regarding the surface wind stress, Figure 5d shows that the Pacific Run produces easterly wind stress anomalies over the equatorial Indian Ocean during the warm phase of the ENSO cycle. Wind anomalies, therefore, oppose the climatological circulation over the region and can lead to warming in the western Indian Ocean and cooling in the eastern Indian Ocean, as suggested by *Webster et al.* [1999]. In the Indo-Pacific Run, the east-west SST anomalies that develop weaken the near-equatorial SST gradient. As a result, the wind stress anomalies introduced by ENSO in the region are amplified in the Indo-Pacific Run. Similar SST-surface heat flux/wind stress relationships are found during the cold phase. Our analyses suggests that both surface heat flux

and surface wind stress contribute to interannual SST variability in the Indian Ocean.

5. Summary and Discussions

[11] This study used a CGCM to examine the impact of the Indian Ocean on the ENSO cycle and its associated ocean–atmosphere fluxes over the Indo-Pacific Ocean region. This is accomplished by comparing CGCM simulations in which SSTs over the latter ocean are either prescribed or determined by interactions with the atmosphere. The results show that the CGCM simulation of ENSO including both the Indian and tropical Pacific Oceans tends to be more realistic than that including the tropical Pacific Ocean only. In particular, the Indo-Pacific Run produces ENSO events with larger amplitude and greater variability on decadal time scales. The interactive Indian Ocean also affects the surface heat flux anomalies in the Indian Ocean during the ENSO cycle and surface wind stress anomalies in both the tropical Indian and Pacific Oceans. The ENSO-related surface heat flux and wind stress anomalies contribute to the interannual variability of the Indian Ocean.

[12] The changes in the ENSO cycle when the Indian Ocean is included are expected as the CGCM can now resolve interannual variability in the Indian Ocean and its interactions with the ENSO cycle. Recent studies [e.g., *Webster et al.*, 1999] suggest that the Indian Ocean can generate its own coupled ocean–atmosphere mode of variability. Interactions between the Indian Ocean coupled mode and ENSO may feedback to affect ENSO characteristics. In addition, since the interactive part of the tropical warm pool covers both the western Pacific Ocean and the eastern Indian Ocean in the Indo-Pacific Run, the eastern Indian Ocean part of the warm pool can respond interactively to Pacific ENSO events. This can amplify the overall feedbacks from the atmosphere during ENSO events.

(a) SHF / Pacific Run (b) Indo-Pacific Run (c) Atlas Data

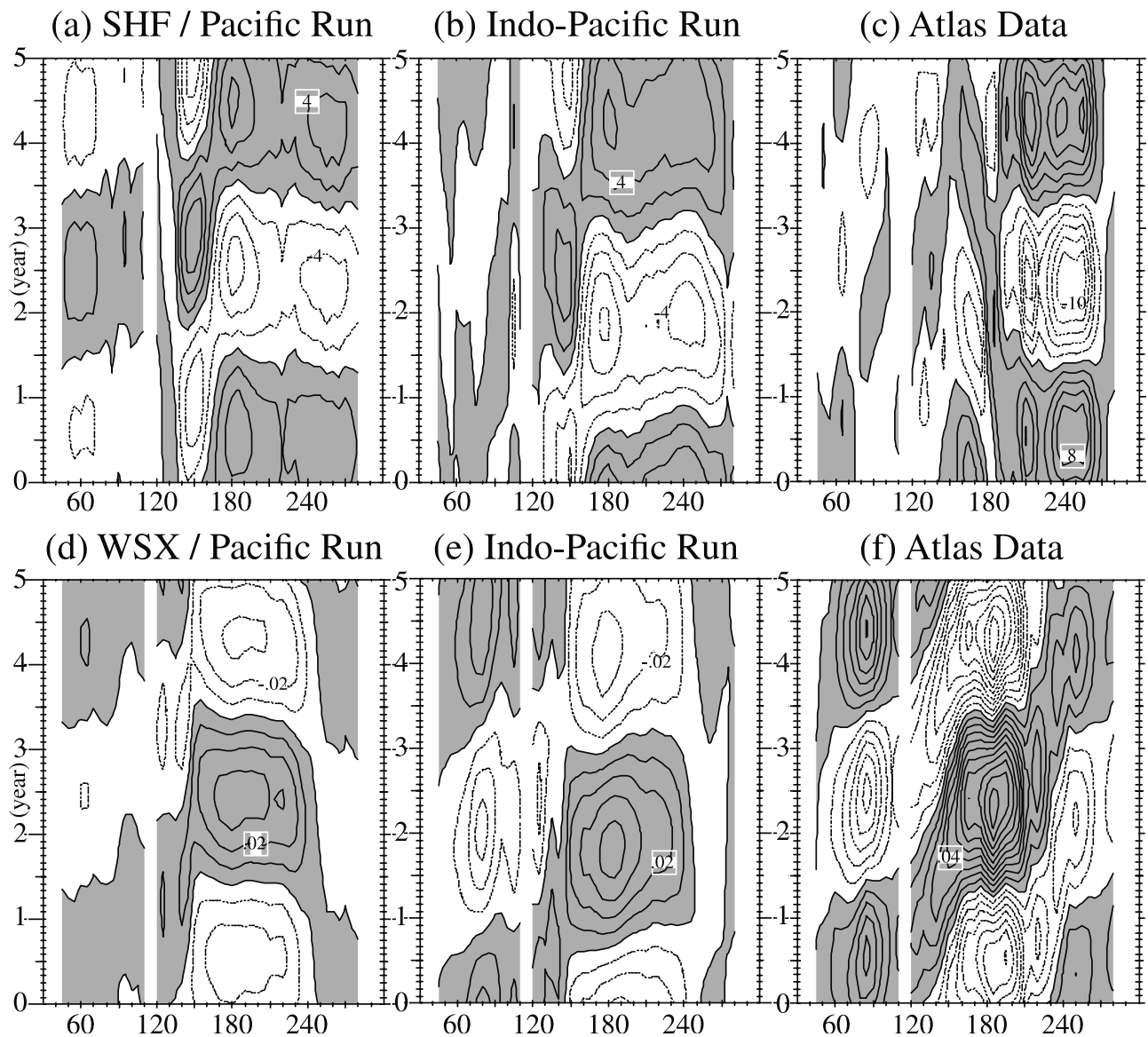## (d) WSX / Pacific Run (e) Indo-Pacific Run (f) Atlas Data

Figure 5. Same as Figure 4, except for surface heat flux anomalies (a–c) and zonal wind stress anomalies (d–f). Contour intervals are 0.01 dyns/cm**2 for zonal wind stress and 2 W/m**2 for surface heat flux.

References

Alexander, R. C., and R. L. Mobley, Monthly average sea-surface temperatures and ice pack limits on a 1 global grid, *Mon. Wea. Rev.*, *104*, 143–148, 1976.

Barnett, T. P., Interaction of the monsoon and Pacific trade wind system at interannual time scales, *Mon. Wea. Rev.*, *112*, 2380–2387, 1984.

da Silva, A., A. C. Young, and S. Levitus, Atlas of Surface Marine Data 1994, Volume 1, Algorithms and Procedures, NOAA Atlas NESDIS 6, U. S. Department of Commerce, Washington, D.C., 1994.

Keppenne, C. L., and M. Ghil, Adaptive Spectral analysis and prediction of the Southern Oscillation Index, *J. Geophys. Res.*, *97*, 20,449–20,454, 1992.

Klein, S. A., B. J. Soden, and N.-C. Lau, Remote sea surface temperature variations during ENSO: Evidence for a tropical atmospheric bridge, *J. Clim.*, *12*, 917–932, 1999.

Lau, N.-C., and M. J. Nath, The role of the "atmospheric bridge" in linking tropical Pacific ENSO events to extratropical SST anomalies, *J. Clim.*, *9*, 2036–2057, 1996.

Meyers, G., Variation of Indonesian throughflow and the El Niño - Southern Oscillation, *J. Geophys. Res.*, *101*, 12,255–12,263, 1996.

Philander, S. G. H., and P. Delecluse, Coastal currents in low latitudes (with application to Somali and El Niño currents), *Deep-Sea Res.*, *30*, 887–902, 1983.

Slutz, R. J., S. J. Lubker, J. D. Hiscox, S. D. Woodruff, R. L. Jenne, D. H.

Joseph, P. M. Steurer, and J. D. Elms, *COADS, Comprehensive Ocean–Atmosphere Data Set, Release 1*, 262 pp., Climate Research Program, Environmental Research Laboratory, Boulder, CO., 1985.

Wainer, I., and P. J. Webster, Monsoon-ENSO interaction using a simple coupled ocean–atmosphere model, *J. Geophys. Res.*, *101*, 25,599–25,614, 1996.

Webster, P. J., S. Yang, I. Wainer, and S. Dixit, Processes Involved in Monsoon Variability, in *Physical Processes in Atmospheric Models*, edited by D. R. Sikka and S. S. Singh, pp. 492–500, Wiley Eastern, New Delhi, 1992.

Webster, P. J., A. Moore, J. Loschnigg, and M. Leban, Coupled ocean–atmosphere dynamics in the Indian Ocean during 1997–98, *Nature*, *40*(23 September), 356–360, 1999.

Woodruff, S. D., R. J. Slutz, R. L. Jenne, and P. M. Steurer, A comprehensive ocean–atmosphere data set, *Bul. Amer. Meteor. Soc.*, *68*, 1239–1250, 1987.

Wyrtki, K., Indonesian throughflow and associated pressure gradient, *J. Geophys. Res.*, *92*, 12,941–12,946, 1987.

Yu, J.-Y., and C. R. Mechoso, A coupled atmosphere-ocean GCM study of the ENSO cycle, *J. Clim.*, *14*, 2329–2350, 2001.

J.-Y. Yu, C. R. Mechoso, J. C. McWilliams, and A. Arakawa, Department of Atmospheric Sciences, University of California Los Angeles, 405 Hilgard Avenue, Los Angeles, CA 90095-1565, USA. (yu@atmos.ucla.edu; mechoso@atmos.ucla.edu; jcm@atmos.ucla.edu; aar@atmos.ucla.edu)